Discontinuous Galerkin Methods for the Time-Harmonic Maxwell Equations

Paul Houston[1], Ilaria Perugia[2], Anna Schneebeli[3], and Dominik Schötzau[4]

[1] Department of Mathematics, University of Leicester, Leicester LE1 7RH, United Kingdom, email: *Paul.Houston@mcs.le.ac.uk*. Supported by the EPSRC (Grant GR/R76615).
[2] Dipartimento di Matematica, Università di Pavia, Via Ferrata 1, 27100 Pavia, Italy, email: *perugia@dimat.unipv.it*.
[3] Department of Mathematics, University of Basel, Rheinsprung 21, 4051 Basel, Switzerland, email: *schneeba@math.unibas.ch*. Supported by the SNSF (Project 21-068126.02).
[4] Mathematics Department, University of British Columbia, Vancouver, BC V6T 1Z2, Canada, email: *schoetzau@math.ubc.ca*.

1 Introduction

In this paper, we review recent work on discontinuous Galerkin (DG) methods for the discretization of the time-harmonic Maxwell equations: find the electric field $\mathbf{u}$ such that

$$\nabla \times (\mu^{-1}\nabla \times \mathbf{u}) - \omega^2(\varepsilon - i\omega^{-1}\sigma)\mathbf{u} = \mathbf{j} \qquad \text{in } \Omega, \tag{1}$$

$$\mathbf{n} \times \mathbf{u} = \mathbf{0} \qquad \text{on } \Gamma = \partial\Omega. \tag{2}$$

Here, Ω is a simply-connected Lipschitz polyhedron in $\mathbb{R}^3$ with connected boundary $\Gamma = \partial\Omega$ and outward normal unit vector $\mathbf{n}$. The function $\mathbf{j}$ is a given source term in $L^2(\Omega)$. The temporal frequency is denoted by $\omega > 0$. The real-valued functions μ, ε and σ are the magnetic permeability, the electric permittivity, and the electric conductivity, respectively.

The main motivation for using a DG approach for the numerical approximation of the above problem is that DG methods, being based on discontinuous finite element spaces, can easily handle meshes with hanging nodes and local spaces of different orders. This renders DG methods ideally suited for *hp*-adaptive algorithms. Moreover, the implementation of discontinuous elements can be based on standard shape functions; a convenience that is particularly advantageous for high-order elements and that is not straightforwardly shared by standard edge elements commonly used in computational electromagnetics (see [1, 3, 14] and the references therein for *hp*-adaptive edge element methods). On the other hand, in the *hp*-context, since most of the degrees of freedom are in the interior of the elements, the increase in the total number of degrees of freedom with respect to the corresponding conforming method is not dramatic.

In this paper, we focus on interior penalty DG discretizations for (1)–(2) in the low-frequency and high-frequency cases (the term $\omega^2\varepsilon$ in (1) is neglected in the former case, whereas the term $i\omega\sigma$ is neglected in the latter).

In the low-frequency case, problem (1)–(2) has to be completed by a divergence-free constraint in the subdomain $\Omega_0 \subseteq \Omega$ covered by insulating material where $\sigma = 0$ (additional scalar constraints arise if $\partial\Omega_0$ is not connected, see, e.g., [13]). This results in the following system:

$$\nabla \times (\mu^{-1}\nabla \times \mathbf{u}) + i\omega\sigma\,\mathbf{u} = \mathbf{j} \quad \text{in } \Omega, \qquad \nabla\cdot(\varepsilon\mathbf{u}) = 0 \quad \text{in } \Omega_0, \qquad \mathbf{n}\times\mathbf{u} = \mathbf{0} \quad \text{on } \Gamma. \tag{3}$$

The main difficulty here is the incorporation of the divergence constraint in the DG framework. Following [8], we show that this can be achieved using a mixed approach where the constraint is accounted for by a suitable Lagrange multiplier. We present the underlying theoretical properties, as well as the energy norm *a priori* and *a posteriori* estimates that were derived in [8] and [6]. For further numerical tests, we also refer to [9].

In the high-frequency case, the problem that consists in finding the electric field $\mathbf{u}$ such that

$$\nabla \times (\mu^{-1} \nabla \times \mathbf{u}) - \omega^2 \varepsilon \mathbf{u} = \mathbf{j} \quad \text{in } \Omega, \qquad \mathbf{n} \times \mathbf{u} = \mathbf{0} \quad \text{on } \Gamma. \tag{4}$$

Here, we assume that ω^2 is not an eigenvalue of the underlying Maxwell eigenproblem. While the design of interior penalty DG methods is straightforward, the key difficulty for (4) arises in the numerical analysis of the methods due to the indefiniteness caused by the zero order term. We present the main results of a novel error analysis that was recently developed in [4]. These results show that DG methods for (4) yield optimal rates of convergence in the energy norm and the L^2-norm. We further present a new set of numerical results on a test problem with a singular solution.

To simplify the presentation in this article, we assume that μ and ε are constants. However, the analysis in [8] covers the case of piecewise smooth material coefficients, whereas the theoretical results in [4] hold for smooth coefficients μ and ε only.

2 Discontinuous Galerkin Discretizations

In this section, we introduce interior penalty DG methods for the two model problems in (3) and (4), and review their theoretical properties.

2.1 Meshes, Trace Operators, Finite Element Spaces and DG Norms

We consider shape-regular affine meshes $\mathcal{T}_h$ that partition the domain Ω into tetrahedra $\{K\}$; the parameter h denotes the mesh size of $\mathcal{T}_h$ given by $h = \max_{K \in \mathcal{T}_h} h_K$, where h_K is the diameter of the element $K \in \mathcal{T}_h$. We denote by $\mathcal{F}_h^{\mathcal{I}}$ the set of all interior faces of elements in $\mathcal{T}_h$, by $\mathcal{F}_h^{\mathcal{B}}$ the set of all boundary faces, and set $\mathcal{F}_h := \mathcal{F}_h^{\mathcal{I}} \cup \mathcal{F}_h^{\mathcal{B}}$. We define the *local meshsize* $\mathtt{h}$ on $\mathcal{F}_h$ by setting $\mathtt{h}(\mathbf{x}) := \max\{h_{K^+}, h_{K^-}\}$, if $\mathbf{x}$ is in the interior of $\partial K^+ \cap \partial K^-$, and by $\mathtt{h}(\mathbf{x}) := h_K$ if $\mathbf{x} \in \partial K$ is on the boundary.

For piecewise smooth vector-valued and scalar-valued functions $\mathbf{v}$ and q, respectively, we introduce the following trace operators. On an interior face $f \in \mathcal{F}_h^{\mathcal{I}}$ shared by two neighboring elements K^+ and K^- with unit outward normal vectors $\mathbf{n}^{\pm}$, respectively, denoting by $\mathbf{v}^{\pm}$ and $q^{\pm}$ the traces of $\mathbf{v}$ and q taken from within $K^{\pm}$, respectively, we define the *jumps* and *averages* across f by $[\![\mathbf{v}]\!]_T := \mathbf{n}^+ \times \mathbf{v}^+ + \mathbf{n}^- \times \mathbf{v}^-$, $[\![q]\!]_N = q^+\mathbf{n}^+ + q^-\mathbf{n}^-$, $\{\!\{\mathbf{v}\}\!\} := (\mathbf{v}^+ + \mathbf{v}^-)/2$ and $\{\!\{q\}\!\} := (q^+ + q^-)/2$, respectively. On a boundary face $f \in \mathcal{F}_h^{\mathcal{B}}$, we set $[\![\mathbf{v}]\!]_T := \mathbf{n} \times \mathbf{v}$, $\{\!\{\mathbf{v}\}\!\} := \mathbf{v}$ and $[\![q]\!]_N = q\mathbf{n}$.

For a given partition $\mathcal{T}_h$ of Ω and an approximation order $\ell \geq 1$, we introduce the following discontinuous finite element spaces:

$$\begin{aligned} \mathbf{V}_h &:= \{\mathbf{v} \in L^2(\Omega)^3 : \mathbf{v}|_K \in \mathcal{P}^\ell(K)^3 \ \ \forall K \in \mathcal{T}_h\}, \\ Q_h &= \{q \in L^2(\Omega)^3 : q|_K \in \mathcal{P}^{\ell+1}(K) \ \ \forall K \in \mathcal{T}_h\}, \end{aligned} \tag{5}$$

where $\mathcal{P}^k(K)$ denotes the space of polynomials of total degree at most k on K.

Finally, denoting by $\| \cdot \|_{s,D}$, for $s \geq 0$ and D a bounded domain in $\mathbb{R}^2$ or $\mathbb{R}^3$, the standard norm in the Sobolev space $H^s(D)^d$, $d \geq 1$, we define the following DG norms with which we will measure the approximation errors:

$$\|\mathbf{v}\|^2_{\mathbf{V}(h)} = \|\varepsilon^{\frac{1}{2}}\mathbf{v}\|^2_{0,\Omega} + \|\mu^{-\frac{1}{2}}\nabla\times\mathbf{v}\|^2_{0,\Omega} + \|\mu^{-\frac{1}{2}}\mathtt{h}^{-\frac{1}{2}}[\![\mathbf{v}]\!]_T\|^2_{0,\mathcal{F}_h},$$
$$\|q\|^2_{Q(h)} = \|\varepsilon^{\frac{1}{2}}\nabla_h q\|^2_{0,\Omega} + \|\varepsilon^{\frac{1}{2}}\mathtt{h}^{-\frac{1}{2}}[\![q]\!]_N\|^2_{0,\mathcal{F}_h}.$$

2.2 DG Discretization of the Low-Frequency Problem (Insulating Materials)

We consider the case of insulating materials, i.e., $\Omega_0 = \Omega$ since all the key difficulties in the numerical treatment of (3) are already present in this particular case. The DG method for the discretization of (3) with $\Omega_0 = \Omega$ and divergence-free source term $\mathbf{j}$ is based on the following mixed formulation of the problem:

$$\begin{aligned} \nabla\times(\mu^{-1}\nabla\times\mathbf{u}) - \varepsilon\nabla p = \mathbf{j} \qquad & \text{in } \Omega,\\ \nabla\cdot(\varepsilon\mathbf{u}) = 0 \qquad & \text{in } \Omega,\\ \mathbf{n}\times\mathbf{u} = \mathbf{0},\ p = 0 \qquad & \text{on } \Gamma. \end{aligned} \tag{6}$$

Here, p is the Lagrange multiplier related to the divergence constraint. The standard variational formulation of (6) is well-posed in $H_0(\mathrm{curl};\Omega)\times H^1_0(\Omega)$; see, e.g., [3, 14].

The mixed DG method for (6) then reads as follows: find $(\mathbf{u}_h, p_h)$ in $\mathbf{V}_h \times Q_h$ such that

$$\begin{aligned} a_h(\mathbf{u}_h,\mathbf{v}) + b_h(\mathbf{v},p_h) &= (\mathbf{j},\mathbf{v}),\\ b_h(\mathbf{u}_h,q) - c_h(p_h,q) &= 0 \end{aligned} \tag{7}$$

for all $(\mathbf{v},q)\in\mathbf{V}_h\times Q_h$, where the discrete forms $a_h(\cdot,\cdot)$, $b_h(\cdot,\cdot)$ and $c_h(\cdot,\cdot)$ are defined, respectively, by

$$\begin{aligned} a_h(\mathbf{u},\mathbf{v}) &= (\mu^{-1}\nabla_h\times\mathbf{u},\nabla_h\times\mathbf{v}) - \int_{\mathcal{F}_h}[\![\mathbf{u}]\!]_T\cdot\{\!\{\mu^{-1}\nabla_h\times\mathbf{v}\}\!\}\,ds\\ &\quad - \int_{\mathcal{F}_h}[\![\mathbf{v}]\!]_T\cdot\{\!\{\mu^{-1}\nabla_h\times\mathbf{u}\}\!\}\,ds + \int_{\mathcal{F}_h}\mathtt{a}\,\mu^{-1}[\![\mathbf{u}]\!]_T\cdot[\![\mathbf{v}]\!]_T\,ds,\\ b_h(\mathbf{v},p) &= -(\varepsilon\mathbf{v},\nabla_h p) + \int_{\mathcal{F}_h}\{\!\{\varepsilon\mathbf{v}\}\!\}\cdot[\![p]\!]_N\,ds,\\ c_h(p,q) &= \int_{\mathcal{F}_h}\mathtt{c}\varepsilon[\![p]\!]_N\cdot[\![q]\!]_N\,ds. \end{aligned}$$

Here, and in the following, we denote by $(\cdot,\cdot)$ the standard inner product in $L^2(\Omega)^d$, $d\geq 1$, and use ∇_h to denote the elementwise application of the operator ∇. Further, we use the notation $\int_{\mathcal{F}_h}\varphi\,ds := \sum_{f\in\mathcal{F}_h}\int_f\varphi\,ds$. The form $a_h(\cdot,\cdot)$ corresponds to the interior penalty discretization of the curl-curl operator, the form $b_h(\cdot,\cdot)$ discretizes the divergence operator in a DG fashion, and the form $c_h(\cdot,\cdot)$ is the interior penalty form that weakly enforces the continuity of p_h.

The parameters $\mathtt{a}$ and $\mathtt{c}$ in $L^\infty(\mathcal{F}_h)$ are the usual *interior penalty stabilization functions* defined by

$$\mathtt{a} := \alpha\,\mathtt{h}^{-1}, \qquad \mathtt{c} := \gamma\,\mathtt{h}^{-1}, \tag{8}$$

where α and γ are positive parameters independent of the mesh size.

The results contained in the following theorem have been proven and numerically validated in [8].

Theorem 1. *There is a parameter $\alpha_{\min} > 0$ only depending on the shape regularity of the mesh and the polynomial approximation degree ℓ such that, for parameters $\alpha > \alpha_{\min}$ and $\gamma > 0$ in (8), the DG method (7) possesses a unique solution.*

Moreover, assume that the analytical solution $(\mathbf{u}, p)$ of (6) satisfies the smoothness assumptions $\varepsilon\mathbf{u} \in H^s(\Omega)^3$, $\mu^{-1}\nabla \times \mathbf{u} \in H^s(\Omega)^3$ and $p \in H^{s+1}(\Omega)$, for an exponent $s > 1/2$, and let $(\mathbf{u}_h, p_h)$ be the DG approximation on conforming meshes defined by (7), with $\alpha > \alpha_{\min}$ and $\gamma > 0$. Then we have the optimal a priori error bound

$$\|\mathbf{u} - \mathbf{u}_h\|_{\mathbf{V}(h)} + \|p - p_h\|_{Q(h)} \leq C\, h^{\min\{s,\ell\}} \left[\|\varepsilon\mathbf{u}\|_{s,\Omega} + \|\mu^{-1}\nabla \times \mathbf{u}\|_{s,\Omega} + \|p\|_{s+1,\Omega}\right],$$

with a constant C independent of the mesh size.

The analysis developed in [8] is valid for *piecewise* smooth coefficients μ and ε and the error estimate in Theorem 1 holds for piecewise smooth solutions. On the other hand, it requires the assumption of conformity of the meshes, although numerical tests in [9] have shown that the method is robust on meshes with hanging nodes as well.

Moreover, the following energy norm *a posteriori* error estimate has been established and tested in [6].

Theorem 2. *We assume that $\nabla \cdot \mathbf{j} = 0$ holds, so that $p \equiv 0$. Let $(\mathbf{u}_h, p_h)$ be the DG approximation on conforming meshes defined by (7), with $\alpha > \alpha_{\min}$ and $\gamma > 0$. Then there is a constant $C > 0$ independent of the mesh size, such that*

$$\|\mathbf{u} - \mathbf{u}_h\|_{\mathbf{V}(h)} + \|p - p_h\|_{Q(h)} \leq C \Big(\sum_{K \in \mathcal{T}_h} \eta_K^2 \Big)^{1/2},$$

where the elemental error indicator η_K is given by

$$\begin{aligned}\eta_K^2 = {} & h_K^{2\sigma}\|\mathbf{j} - \nabla \times (\mu^{-1}\nabla \times \mathbf{u}_h) + \varepsilon\nabla p_h\|_{0,K}^2 + h_K^{2\sigma-1}\|\widehat{\tau}_K(\mathbf{u}_h) - \tau_K(\mathbf{u}_h)\|_{0,\partial K}^2 \\ & + h_K^{-1}\|\mu^{\frac{1}{2}}[\![\mathbf{u}_h]\!]_T\|_{0,\partial K}^2 + h_K\|[\![\varepsilon\mathbf{u}_h]\!]_N\|_{0,\partial K \setminus \Gamma}^2 + h_K^2\|\nabla \cdot (\varepsilon\mathbf{u}_h)\|_{0,K}^2 \\ & + \|\varepsilon^{\frac{1}{2}}\nabla p_h\|_{0,K}^2 + h_K^{-1}\|\varepsilon^{\frac{1}{2}}[\![p_h]\!]_N\|_{0,\partial K}^2,\end{aligned}$$

$\sigma \in (1/2, 1]$ is the parameter of the embeddings $H_0(\mathrm{curl}; \Omega) \cap H(\mathrm{div}; \Omega) \hookrightarrow H^\sigma(\Omega)^3$ and $H(\mathrm{curl}; \Omega) \cap H_0(\mathrm{div}; \Omega) \hookrightarrow H^\sigma(\Omega)^3$ (see [2]), and $\widehat{\tau}_K(\mathbf{v})$ is the numerical flux *defined by*

$$\widehat{\tau}_K(\mathbf{v}) = \begin{cases} \mathbf{n}_K \times (\{\!\{\mu^{-1}\nabla \times \mathbf{v}\}\!\} - \mu^{-1}\mathtt{a}\,[\![\mathbf{v}]\!]_T) & \text{on } \partial K \setminus \Gamma, \\ \mathbf{n}_K \times (\mu^{-1}\nabla \times \mathbf{v} - \mu^{-1}\mathtt{a}\,(\mathbf{n}_K \times \mathbf{v})) & \text{on } \partial K \cap \Gamma. \end{cases}$$

2.3 DG Discretization of the High-Frequency Problem

For problem (4), the interior penalty DG method is given by: find $\mathbf{u}_h \in \mathbf{V}_h$ such that

$$a_h(\mathbf{u}_h, \mathbf{v}) - \omega^2(\varepsilon\mathbf{u}_h, \mathbf{v}) = (\mathbf{j}, \mathbf{v}) \tag{9}$$

for all $\mathbf{v} \in \mathbf{V}_h$, where the discrete form $a_h(\cdot,\cdot)$ is the same as in Section 2.2. The *interior penalty stabilization function* $\mathtt{a} \in L^\infty(\mathcal{F}_h)$ is defined again by (8), with α chosen independently of the mesh size and the frequency.

The following *a priori* error estimates in the energy norm and in the L^2-norm have been proven in [4]. Their proof is based on techniques similar to those of [12] and [11, Section 7.2], for the energy error bound, and of [10, Theorem 3.2], for the L^2-error bound, combined with novel results that allow one to approximate a discontinuous function by a conforming one. This result is instrumental in controlling the non-conformity of the DG method.

Theorem 3. *Assume that the analytical solution* $\mathbf{u}$ *of (4) satisfies the regularity assumptions* $\varepsilon\mathbf{u} \in H^s(\Omega)^3$ *and* $\mu^{-1}\nabla \times \mathbf{u} \in H^s(\Omega)^3$, *for* $s > \frac{1}{2}$, *and let* $\mathbf{u}_h$ *be the DG approximation on conforming meshes defined by (9). Then there is a parameter* $\alpha_{\min} > 0$ *only depending on the shape regularity of the mesh and on the polynomial approximation degree* ℓ, *and a mesh size* $h_0 > 0$ *such that, for* $\alpha \geq \alpha_{\min}$ *and* $0 < h \leq h_0$, *we have the optimal a priori error bound*

$$\|\mathbf{u} - \mathbf{u}_h\|_{\mathbf{V}(h)} \leq C\, h^{\min\{s,\ell\}} \Big[\|\varepsilon\mathbf{u}\|_{s,\Omega} + \|\mu^{-1}\nabla \times \mathbf{u}\|_{s,\Omega} \Big],$$

with a constant $C > 0$ *independent of the mesh size.*

Consequently, for $\alpha \geq \alpha_{\min}$, *the DG method (9) admits a unique solution* $\mathbf{u}_h \in \mathbf{V}_h$, *provided that* $h \leq h_0$.

Finally, assume that the analytical solution $\mathbf{u}$ *of (4) satisfies the additional regularity assumption* $\mathbf{u} \in H^{s+\sigma}(\Omega)^3$ *for* $s > \frac{1}{2}$ *and* $\sigma \in (1/2, 1]$ *the parameter of the embeddings* $H_0(\mathrm{curl};\Omega) \cap H(\mathrm{div};\Omega) \hookrightarrow H^\sigma(\Omega)^3$ *and* $H(\mathrm{curl};\Omega) \cap H_0(\mathrm{div};\Omega) \hookrightarrow H^\sigma(\Omega)^3$ *(see [2]). Then, for* $\alpha \geq \alpha_{\min}$, *there is a mesh size* $h_2 > 0$ *such that, for* $0 < h \leq h_2$, *we have*

$$\|\varepsilon^{\frac{1}{2}}(\mathbf{u} - \mathbf{u}_h)\|_{0,\Omega} \leq C\, h^{\min\{s,\ell\}+\sigma} \Big[\|\varepsilon\mathbf{u}\|_{s+\sigma,\Omega} + \|\mu^{-1}\nabla \times \mathbf{u}\|_{s,\Omega} \Big],$$

with a constant $C > 0$ *independent of the mesh size.*

The analysis of [4] is based on duality arguments; thus, the result of Theorem 3 can easily be extended to smooth material coefficients μ and ε. However, the extension to piecewise smooth coefficients requires alternative mathematical tools; this is the subject of ongoing research.

3 Numerical Example

In this section we present a numerical example to highlight the practical performance of the DG method introduced and analyzed in this article for the numerical approximation of the high-frequency indefinite time-harmonic Maxwell equations in (4), considering a model problem with a singular solution. Throughout this section, we take $\mu = \mu_0$ and $\varepsilon = \varepsilon_0$, the permeability and permittivity of the free space, respectively, and select the interior penalty parameter α in (8) as follows: $\alpha = 10\,\ell^2$. As is standard in electromagnetic computations, we scale the electric field by $\mathbf{u} \to \mu_0\mathbf{u}$ and obtain a problem for the scaled field (that we again denote by $\mathbf{u}$) of the form

$$\nabla \times \nabla \times \mathbf{u} - k^2\mathbf{u} = \mathbf{j} \quad \text{in } \Omega, \qquad \mathbf{n} \times \mathbf{u} = \mathbf{0} \quad \text{on } \Gamma, \tag{10}$$

with a rescaled right-hand side (again denoted by $\mathbf{j}$) and the wave number $k = \omega\sqrt{\mu_0\varepsilon_0}$.

For simplicity, we restrict ourselves to the two-dimensional analogue of (10). To this end, we let Ω be the L-shaped domain $(-1,1)^2 \setminus [0,1) \times (-1,0]$ and select $\mathbf{j}$ (and suitable non-homogeneous boundary conditions for $\mathbf{u}$) so that the analytical solution $\mathbf{u}$ to the two-dimensional analogue of (10) is given, in terms of the polar coordinates (r,ϑ), by

$$\mathbf{u}(x,y) = \nabla S(r,\vartheta), \quad \text{where} \quad S(r,\vartheta) = (kr)^{2/3}\sin(2\vartheta/3). \tag{11}$$

Here, the boundary conditions are enforced in the usual DG manner by adding boundary terms in the formulation (9); see [5, 7] for details. The analytical solution given by (11)

Table 1. Convergence of $\|\mathbf{u}-\mathbf{u}_h\|_{\mathbf{V}(h)}$ with $k=1$.

	$\ell=1$		$\ell=2$		$\ell=3$	
Elements	$\|\mathbf{u}-\mathbf{u}_h\|_{\mathbf{V}(h)}$	r	$\|\mathbf{u}-\mathbf{u}_h\|_{\mathbf{V}(h)}$	r	$\|\mathbf{u}-\mathbf{u}_h\|_{\mathbf{V}(h)}$	r
24	1.525e-1	-	8.881e-2	-	6.078e-2	-
96	8.875e-2	0.78	5.374e-2	0.73	3.744e-2	0.70
384	5.393e-2	0.72	3.331e-2	0.69	2.337e-2	0.68
1536	3.348e-2	0.69	2.085e-2	0.68	1.467e-2	0.67
6144	2.096e-2	0.68	1.310e-2	0.67	9.227e-3	0.67

then contains a singularity at the re-entrant corner located at the origin of Ω; in particular, we note that $\mathbf{u}$ lies in the Sobolev space $H^{2/3-\varepsilon}(\Omega)^2$, $\varepsilon>0$. This example represents a slight modification of the numerical experiment presented in [4]; cf., also, [1].

We investigate the asymptotic convergence of the DG method on a sequence of successively finer (quasi-uniform) unstructured triangular meshes for $\ell=1,2,3$ as the wave number k increases. To this end, in Tables 1, 2, 3 and 4 we present numerical experiments for $k=1,2,4,6$, respectively. In each case we show the number of elements in the computational mesh, the corresponding DG-norm of the error $\|\mathbf{u}-\mathbf{u}_h\|_{\mathbf{V}(h)}$ and the numerical rate of convergence r. In view of the scaling we introduced, we have taken $\|\mathbf{u}-\mathbf{u}_h\|_{\mathbf{V}(h)}$ as $\left(\|\mathbf{u}-\mathbf{u}_h\|_{0,\Omega}^2+\|\nabla\times(\mathbf{u}-\mathbf{u}_h)\|_{0,\Omega}^2+\|\mathrm{h}^{-\frac{1}{2}}[\![\mathbf{u}-\mathbf{u}_h]\!]_T\|_{0,\mathcal{F}_h}^2\right)^{\frac{1}{2}}$. We observe that (asymptotically) $\|\mathbf{u}-\mathbf{u}_h\|_{\mathbf{V}(h)}$ converges to zero at the optimal rate $\mathcal{O}(h^{2/3-\varepsilon})$, for each fixed ℓ and each k, as h tends to zero, as predicted by Theorem 3. In particular, we make two key observations: firstly, we note that for a given fixed mesh and fixed polynomial degree, an increase in the wave number k leads to an increase in the DG-norm of the error in the approximation to $\mathbf{u}$ As pointed out in [1], where curl-conforming finite element methods were employed for the numerical approximation of (10), the pre-asymptotic region increases as k increases; this is particularly evident when $k=6$, cf. Table 4. Secondly, we observe that the DG-norm of the error decreases when either the mesh is refined, or the polynomial degree is increased as we would expect; this is also the case when the DG-norm of the error is compared with the total number of degrees of freedom employed in the underlying finite element space, for each fixed k; for brevity these results have been omitted.

Finally, we end this section by considering the rate of convergence of the error in the approximation to $\mathbf{u}$ measured in the L^2-norm. While for smooth solutions the optimal L^2-order has been confirmed numerically (see [4]), the additional regularity assumptions for the L^2 estimate in Theorem 3 do not hold in the example considered here. Notwithstanding this, in Figure 1 we plot the L^2-norm of the error in the approximation to $\mathbf{u}$, with the square root of the number of degrees of freedom in the finite element space $\mathbf{V}_h$, for $k=1$ and $k=6$. We observe that (asymptotically) $\|\mathbf{u}-\mathbf{u}_h\|_{0,\Omega}$ converges to zero at the rate $\mathcal{O}(h^{2/3})$, for each fixed ℓ and k, as in the case of the DG-norm of the error.

4 Conclusions

In this paper, we have reviewed two interior penalty discontinuous Galerkin methods for the numerical approximation of the time-harmonic Maxwell equations in both the low-

Table 2. Convergence of $\|\mathbf{u}-\mathbf{u}_h\|_{\mathbf{V}(h)}$ with $k=2$.

	$\ell=1$		$\ell=2$		$\ell=3$	
Elements	$\|\mathbf{u}-\mathbf{u}_h\|_{\mathbf{V}(h)}$	r	$\|\mathbf{u}-\mathbf{u}_h\|_{\mathbf{V}(h)}$	r	$\|\mathbf{u}-\mathbf{u}_h\|_{\mathbf{V}(h)}$	r
24	2.272e-1	-	1.366e-1	-	9.490e-2	-
96	1.369e-1	0.73	8.428e-2	0.70	5.904e-2	0.69
384	8.464e-2	0.69	5.262e-2	0.68	3.700e-2	0.67
1536	5.290e-2	0.68	3.303e-2	0.67	2.326e-2	0.67
6144	3.322e-2	0.67	2.078e-2	0.67	1.464e-2	0.67

Table 3. Convergence of $\|\mathbf{u}-\mathbf{u}_h\|_{\mathbf{V}(h)}$ with $k=4$.

	$\ell=1$		$\ell=2$		$\ell=3$	
Elements	$\|\mathbf{u}-\mathbf{u}_h\|_{\mathbf{V}(h)}$	r	$\|\mathbf{u}-\mathbf{u}_h\|_{\mathbf{V}(h)}$	r	$\|\mathbf{u}-\mathbf{u}_h\|_{\mathbf{V}(h)}$	r
24	8.727e-1	-	3.900e-1	-	2.274e-1	-
96	3.637e-1	1.26	1.853e-1	1.07	1.156e-1	0.98
384	1.793e-1	1.02	9.786e-2	0.92	6.462e-2	0.84
1536	9.670e-2	0.89	5.622e-2	0.80	3.845e-2	0.75
6144	5.611e-2	0.79	3.395e-2	0.73	2.363e-2	0.70

Table 4. Convergence of $\|\mathbf{u}-\mathbf{u}_h\|_{\mathbf{V}(h)}$ with $k=6$.

	$\ell=1$		$\ell=2$		$\ell=3$	
Elements	$\|\mathbf{u}-\mathbf{u}_h\|_{\mathbf{V}(h)}$	r	$\|\mathbf{u}-\mathbf{u}_h\|_{\mathbf{V}(h)}$	r	$\|\mathbf{u}-\mathbf{u}_h\|_{\mathbf{V}(h)}$	r
24	2.535	-	8.535e-1	-	6.884e-1	-
96	7.305e-1	1.79	5.972e-1	0.52	2.048e-1	1.75
384	3.230e-1	1.18	1.641e-1	1.86	1.002e-1	1.03
1536	1.879e-1	0.78	8.383e-2	0.97	5.461e-2	0.88
6144	8.275e-2	1.18	4.722e-2	0.83	3.207e-2	0.77

frequency and high-frequency regimes. The predicted performance of the DG method for the indefinite problem in the high-frequency case has been confirmed in a new set of numerical experiments carried out on a model problem with a singular solution.

References

1. M. Ainsworth and J. Coyle. Hierarchic *hp*-edge element families for Maxwell's equations on hybrid quadrilateral/triangular meshes. *Comput. Methods Appl. Mech. Engrg.*, 190:6709–6733, 2001.
2. C. Amrouche, C. Bernardi, M. Dauge, and V. Girault. Vector potentials in three-dimensional non-smooth domains. *Math. Models Appl. Sci.*, 21:823–864, 1998.
3. L. Demkowicz and L. Vardapetyan. Modeling of electromagnetic absorption/scattering problems using *hp*–adaptive finite elements. *Comput. Methods Appl. Mech. Engrg.*, 152:103–124, 1998.

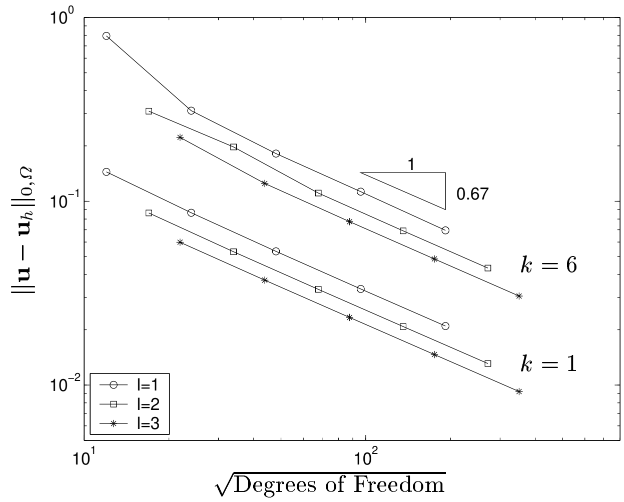

Fig. 1. Convergence of $\|\mathbf{u}-\mathbf{u}_h\|_{0,\Omega}$ for $k=1$ and $k=6$.

4. P. Houston, I. Perugia, A. Schneebeli, and D. Schötzau. Interior penalty method for the indefinite time-harmonic maxwell equations. Technical Report PIMS-03-15, Pacific Institute for the Mathematical Sciences, Universify of British Columbia, 2003.
5. P. Houston, I. Perugia, and D. Schötzau. Mixed discontinuous Galerkin approximation of the Maxwell operator. Technical Report 02-16, University of Basel, Department of Mathematics, 2002. Accepted for publication in *SIAM J. Numer. Anal.*
6. P. Houston, I. Perugia, and D. Schötzau. Energy norm a posteriori error estimation for mixed discontinuous Galerkin approximations of the Maxwell operator. Technical Report 2003/16, University of Leicester, Department of Mathematics, 2003.
7. P. Houston, I. Perugia, and D. Schötzau. *hp*-DGFEM for Maxwell's equations. In F. Brezzi, A. Buffa, S. Corsaro, and A. Murli, editors, *Numerical Mathematics and Advanced Applications ENUMATH 2001*, pages 785–794. Springer-Verlag, 2003.
8. P. Houston, I. Perugia, and D. Schötzau. Mixed discontinuous Galerkin approximation of the Maxwell operator: Non-stabilized formulation. Technical Report 2003/17, University of Leicester, Department of Mathematics, 2003.
9. P. Houston, I. Perugia, and D. Schötzau. Nonconforming mixed finite element approximations to time-harmonic eddy current problems. Technical Report 2003/15, University of Leicester, Department of Mathematics, 2003.
10. P. Monk. A finite element method for approximating the time-harmonic Maxwell equations. *Numer. Math.*, 63:243–261, 1992.
11. P. Monk. *Finite element methods for Maxwell's equations.* Oxford University Press, New York, 2003.
12. P. Monk. A simple proof of convergence for an edge element discretization of Maxwell's equations. In C. Carstensen, S. Funken, W. Hackbusch, R. Hoppe, and P. Monk, editors, *Computational electromagnetics*, volume 28 of *Lect. Notes Comput. Sci. Engrg.*, pages 127–141. Springer–Verlag, 2003.
13. I. Perugia and D. Schötzau. The *hp*-local discontinuous Galerkin method for low-frequency time-harmonic Maxwell equations. *Math. Comp.*, 72:1179–1214, 2003.
14. L. Vardapetyan and L. Demkowicz. *hp*-adaptive finite elements in electromagnetics. *Comput. Methods Appl. Mech. Engrg.*, 169:331–344, 1999.